Open

Molecular Psychiatry (2010) 15, 823–830

www.nature.com/mp

ORIGINAL ARTICLE

Medial prefrontal cortex pathology in schizophrenia as revealed by convergent findings from multimodal imaging

E Pomarol-Clotet[1,2], EJ Canales-Rodríguez[1,2], R Salvador[1,2], S Sarró[1,2,3], JJ Gomar[1,2], F Vila[4], J Ortiz-Gil[1,2], Y Iturria-Medina[5], A Capdevila[4,6] and PJ McKenna[1,2]

[1]*Benito Menni Complex Assistencial en Salut Mental, Barcelona, Spain;* [2]*CIBERSAM, Spain;* [3]*Psychiatry and Clinical Psychology Programme, Universitat Autònoma de Barcelona, Barcelona, Spain;* [4]*Fundació Sant Joan de Déu, Barcelona, Spain;* [5]*Neuroimaging Department, Cuban Neuroscience Center, Havana, Cuba and* [6]*CIBER-BBN, Spain*

Neuroimaging studies have found evidence of altered brain structure and function in schizophrenia, but have had complex findings regarding the localization of abnormality. We applied multimodal imaging (voxel-based morphometry (VBM), functional magnetic resonance imaging (fMRI) and diffusion tensor imaging (DTI) combined with tractography) to 32 chronic schizophrenic patients and matched healthy controls. At a conservative threshold of $P = 0.01$ corrected, structural and functional imaging revealed overlapping regions of abnormality in the medial frontal cortex. DTI found that white matter abnormality predominated in the anterior corpus callosum, and analysis of the anatomical connectivity of representative seed regions again implicated fibres projecting to the medial frontal cortex. There was also evidence of convergent abnormality in the dorsolateral prefrontal cortex, although here the laterality was less consistent across techniques. The medial frontal region identified by these three imaging techniques corresponds to the anterior midline node of the default mode network, a brain system which is believed to support internally directed thought, a state of watchfulness, and/or the maintenance of one's sense of self, and which is of considerable current interest in neuropsychiatric disorders.
Molecular Psychiatry (2010) **15,** 823–830; doi:10.1038/mp.2009.146; published online 12 January 2010

Keywords: schizophrenia; voxel-based morphometry; fMRI; diffusion tensor imaging; default mode network; anterior cingulate cortex

Introduction

Among the many lines of investigation undertaken to characterize the brain pathology of schizophrenia, one of the most productive has been neuroimaging. Early studies using computed tomography established beyond doubt that there is lateral ventricular enlargement in the disorder,[1] and magnetic resonance imaging (MRI) studies have shown that this is coupled with a small degree of brain tissue volume reduction of around 2%.[2] MRI studies have also suggested that brain volume loss in schizophrenia, although widespread, is not homogeneous, but is instead most pronounced in medial temporal lobe structures[2] and in the grey matter of the superior temporal cortex.[3] Recent studies using voxel-based morphometry (VBM), which identifies clusters of difference between groups of subjects in an unbiased way without the necessity of preselecting regions of interest, have confirmed that cortical grey matter volume reductions are prominent in parts of the temporal lobe cortex.[4] However, these studies have also found evidence of volume reductions in other areas, including the anterior cingulate cortex, insular cortex, left middle frontal gyrus and postcentral gyrus.[5]

Although structural imaging has implicated a variety of brain regions in schizophrenia, the emphasis in functional imaging studies has been and continues to be on the frontal lobes. The original functional imaging finding of hypofrontality, although not consistently replicated, has been supported by meta-analysis both at rest and under conditions of neuropsychological task activation.[6] At the same time, it is increasingly clear that the prefrontal cortex dysfunction in schizophrenia goes beyond any simple concept of hypofunction. Thus, rather than hypofrontality, a number of studies have found evidence of increased activation in the prefrontal cortex during performance of working memory tasks.[7–10] This 'hyperfrontality' has been found in the dorsolateral and ventral prefrontal regions, and whether it is seen seems to depend on the nature of

Correspondence: Dr E Pomarol-Clotet, Research unit, Benito Menni Complex Assistencial en Salut Mental, Germanes Hospitalàries del Sagrat Cor de Jesús, C/Dr Antoni Pujadas 38-C, Sant Boi de Llobregat, Barcelona 08830, Spain.
E-mail: edith.pomarol@gmail.com
Received 21 August 2009; revised 8 November 2009; accepted 24 November 2009; published online 12 January 2010

the task used, and how well the patients perform it.[9–13] Complicating matters further, two recent studies have found that schizophrenic patients show a failure of task-related deactivation in the medial frontal cortex.[14,15] This medial frontal area corresponds to part of the so-called default mode network, a series of interconnected regions that are highly active at rest but which deactivate during performance of a wide range of cognitive tasks.[16]

A third imaging technique that is increasingly being applied to schizophrenia is diffusion tensor imaging (DTI). This indexes white matter abnormality by means of decreased fractional anisotropy (FA);[17] tractography algorithms can also be used to identify which particular tracts are affected. Over 20 studies have indicated that schizophrenia is associated with decreased FA, particularly in the white matter tracts connecting temporal and prefrontal regions. However, to date there is a lack of convergence in the findings, and the majority of studies have used a region-of-interest (ROI) approach rather than whole-brain-based examination.[17]

It has been suggested that further understanding of brain pathology in schizophrenia will depend on the integration of findings from voxel-based structural techniques with those from functional imaging and white matter tractography using DTI.[18] To date, however, relatively few such 'multimodal' imaging studies have been carried out, and these have either used only two imaging techniques[19–21] or have focused on discrete brain structures such as the hippocampus and amygdala.[22–24] In this study, we report for the first time the use of a whole-brain approach combining all three imaging modalities, to determine what, if any, common sites of pathology they identify in the disorder.

Methods

Subjects

The patient sample consisted of 32 schizophrenic patients recruited from two hospitals. They all met Diagnostic and Statistical Manual of Mental Disorders, 4th Edition (DSM-IV) criteria for schizophrenia, based on interview and review of clinical history. Patients were excluded if (a) they were <18 or >65 years of age, (b) had a history of brain trauma or neurological disease and (c) had shown alcohol/substance abuse within 12 months before participation. Altogether, 27 were in-patients and 5 were living outside the hospital with relatives or in supported accommodation. They all had chronic illnesses (range 5–39 years), were symptomatic (mean Positive and Negative Symptoms Scale (PANSS) score 71.97 ± 17.01) and had on an average moderately severe illness (Global Assessment of Function score $= 44.03 \pm 10.89$). They were all scanned when in relatively stable condition (that is, outside any period of acute relapse). All were taking neuroleptic medication (clozapine $N=7$, other atypicals $N=10$, typical neuroleptics $N=3$, combined typical and atypical treatment $N=12$). Functional MRI (fMRI) findings on this sample have previously been described by Pomarol-Clotet *et al*.[14]

The controls consisted of 32 healthy individuals selected to be age- and sex-matched to the patients and meeting the same exclusion criteria. Subjects were recruited from nonmedical staff working in the hospital, their relatives and acquaintances, and also from independent sources in the community. They were questioned and excluded if they reported a history of mental illness and/or treatment with psychotropic medication. Written informed consent was obtained from all participants. The study was approved by the local hospital ethics committee.

Procedure

All subjects underwent structural and functional MRI scanning in a single session, using the same 1.5 T GE Signa scanner (General Electric Medical Systems, Milwaukee, WI, USA), at the Sant Joan de Déu Hospital in Barcelona (Spain).

Structural imaging. High-resolution structural T1 MRI data were acquired with the following acquisition parameters: matrix size 512×512; 180 contiguous axial slices; voxel resolution $0.47 \times 0.47 \times 1\,\text{mm}^3$; echo (TE), repetition (TR) and inversion (TI) times, (TE/TR/TI) = 3.93 ms/2000 ms/710 ms, respectively; flip angle 15°.

Structural data were analysed with FSL-VBM, an optimized VBM style analysis[25,26] carried out with FMRIB Software Library (FSL) tools;[27] this yields a measure of difference in the local grey matter volume. In a first step, structural images were brain-extracted using BET.[28] Next, tissue-type segmentation was carried out and the resulting grey matter partial volume images were aligned to the MNI152 standard space using the FSL tools FLIRT and FNIRT. The resulting images were averaged to create a study-specific template, to which the native grey matter images were nonlinearly re-registered. These images were modulated (to correct for local expansion or contraction) by dividing by the Jacobian of the warp field, and they were later smoothed with an isotropic Gaussian kernel with a sigma of 4 mm. Finally, group comparisons between patients and controls were carried out with permutation-based nonparametric tests. These were made with the *randomize* function implemented in FSL, using the recently developed threshold-free cluster-enhancement method, for proper statistical inference of spatially distributed patterns.[29]

fMRI. The paradigm used has been described in Pomarol-Clotet *et al*.[14] Scanning was carried out while participants performed a sequential-letter version of the *n*-back task.[30] Two levels of memory load (1- and 2-back) were presented in a block design manner. Each block consisted of 24 letters that were shown every 2 s (1 s on, 1 s off) and all blocks contained 5 repetitions (1- and 2-back depending on the block) located randomly within block. Individuals

had to detect them and inform by pressing a button. Four 1-back and four 2-back blocks were presented in an interleaved way, and between them, a baseline stimulus (an asterisk flashing with the same frequency as the letters) was always presented for 16 s. To identify which task had to be performed, characters were shown in green in 1-back blocks and in red in the 2-back blocks. All participants first went through a training session, outside the scanner.

In each individual scanning session 266 volumes were acquired. A gradient-echo echo-planar (EPI) sequence depicting the blood-oxygenation-level-dependent (BOLD) contrast was used. Each volume contained 16 axial planes acquired with the following parameters: TR = 2000 ms, TE = 20 ms, flip angle = 70°, section thickness = 7 mm, section skip = 0.7 mm, in-plane resolution = $3 \times 3\,mm^2$. The first 10 volumes were discarded to avoid T1 saturation effects.

Functional MRI image analyses were performed with the fMRI Expert Analysis Tool (FEAT) module, included in the FSL software. At a first level, images were corrected for movement, were coregistered to a common stereotaxic space (Montreal Neurologic Institute template) and were spatially smoothed with a Gaussian filter (FWHM = 5 mm). To minimize unwanted movement-related effects, individuals with an estimated maximum absolute movement over 3.0 mm, or an average absolute movement higher than 0.3 mm were discarded from the study. Finally, group comparisons between patients and controls were performed using the same FEAT module, by means of mixed-effects GLM models. A *z*-threshold of 2.3 (the default in FSL) was used to generate the initial set of clusters. FEAT uses the Gaussian Random Field theory to properly account for the spatially distributed patterns when performing statistical tests.

DTI. The whole brain diffusion-weighted images were recorded along 25 gradient directions using three different *b*-values (500, 750 and 1000 $s\,mm^{-2}$) together with three unweighted ($b = 0$) images (78 images in total). For each image, we used the following parameters: field of view = $289 \times 289\,mm^2$; matrix size 128×128; number of slices 28; voxel resolution $1.13 \times 1.13 \times 5\,mm^3$; TE = 107 ms; TR = 8000 ms.

The DTI data sets were analysed with FSL-TBSS,[26] a Tract-Based Spatial Statistics analysis carried out with FSL tools. In a first step, FA images were created by fitting a tensor model to the raw diffusion data using FMRIB's Diffusion Toolbox (FDT), and then brain-extracted using BET.[28] All subjects' FA data were then aligned into a common space using the nonlinear registration tool FNIRT (Andersson *et al.*[31]; Andersson *et al.*[32]), which uses a b-spline representation of the registration warp field.[33] Next, the mean FA image was created and thinned to create a mean FA skeleton, which represents the centres of all tracts common to the group. Each subject's aligned FA data were then projected onto this skeleton. As in the VBM analysis, group comparisons between patients and controls were performed using the *randomize* function implemented in FSL, which carries out permutation-based, nonparametric comparisons.

In addition, the output from the DTI analysis was used to explore the potential differences in white matter structural connectivity. For this we used the voxel-based methodology described by Iturria-Medina *et al.*,[34,35] which uses Dijkstra's graph theory algorithm to find the most probable route of connection between any pairs of voxels in the brain. First, the statistical map resulting from TBSS was automatically partitioned into nonoverlapping clusters. Next, four of these clusters were selected as representative ROIs, after considering their central location in each of the significant tracts, and avoiding other clusters containing fibre intersections (which would make the interpretation of results difficult). Every ROI was used separately as a seed mask by an optimized tractography algorithm,[34] delivering three-dimensional images that quantified the degree of anatomical connection between a particular ROI and each voxel in the brain.[35] Finally, all individual maps were aligned into a common space and they were smoothed with an isotropic Gaussian kernel with a sigma of 4 mm. This allowed comparing connectivity patterns between patients and controls using the same permutation-based *randomize* function from FSL.

Statistical thresholds

In the three principal analyses comparing patients and controls, a threshold of $P = 0.01$, corrected for multiple comparisons across space, was used. We applied this relatively conservative threshold in order to minimize false-positive findings arising from the analysis of several modalities and from different sets of images. Using this threshold on the three main comparisons leads to an overall probability of finding one (or more) false positive of 0.03. Results applying a corrected $P = 0.05$ in the individual tests are reported in the Supplementary Material. However, these results should be treated with caution, as they imply an overall probability of 0.14 for false positives in the three main comparisons.

Results

Demographic findings

Demographic findings are shown in Table 1. The patients and controls were selected to be matched for age and sex. There were also no significant differences between their score on the Word Accentuation Test (Test de Acentuación de Palabras, TAP), a test designed to estimate intelligence quotient (IQ) (premorbid IQ in the patients) analogous to the National Adult Reading Test in English,[36] on the basis of pronunciation of low-frequency Spanish words whose accents are removed.[37] As typically found in schizophrenia, the patients, however, had a lower current IQ than the controls.

Table 1 Demographic characteristics of patients and controls

	Patients (n = *32*)	*Controls* (n = *32*)	P-*value*
Age	41.56 ± 8.79 (28–60)	41.03 ± 11.04 (range 21–59)	0.83
Sex (M/F)	21/11	21/11	1
TAP correct words	21.55 ± 5.58	22.93 ± 4.63	0.32
Current IQ (WAIS-III)	94.31 ± 9.02 (range 80–110)	100.52 ± 9.10 (range 80–110)	0.01
Duration of illness (years)	21.79 ± 9.09 (range 5–39)	—	—
GAF score	44.03 ± 10.89 (range 22–65)	—	—
PANSS score	71.97 ± 17.01 (range 38–116)	—	—

Abbreviations: F, female; GAF, Global Assessment of Function; IQ, intelligence quotient; M, male; WAIS, Wechsler Adult Intelligence Scale.

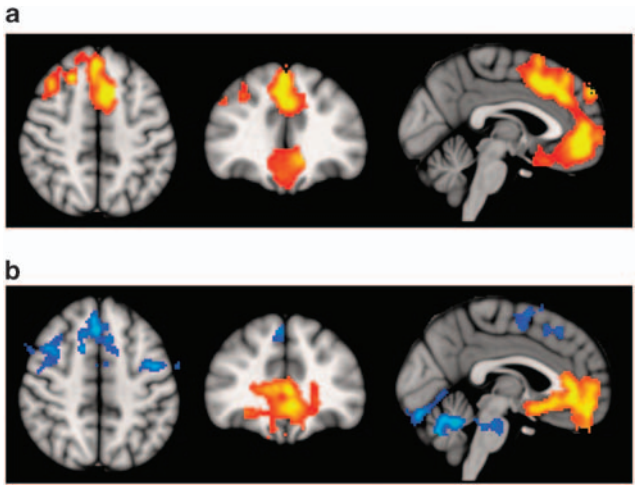

Figure 1 Top panel: (**a**) voxel-based morphometry (VBM) findings. Regions showing significant volume reduction thresholded at $P = 0.01$ in the schizophrenic patients are shown in orange. Bottom panel: (**b**) functional magnetic resonance imaging (fMRI) findings. Regions are shown where there were significant differences between patients and controls during performance of the *n*-back task (2-back vs baseline comparison), thresholded at $P = 0.01$. Blue indicates hypoactivation, that is, areas where controls activated significantly more than the patients. Orange indicates areas where the schizophrenic patients showed failure to deactivate in comparison to controls. The right side of the images represents the left side of the brain.

VBM

Because of poor image quality, two individuals (1 control and 1 patient) were excluded from the VBM analyses. At a $P = 0.01$, only two areas of the brain showed significant differences in volume between patients and controls (see Figure 1a). One of these was centred in the medial frontal cortex (peak in Brodmann area 32 (BA 32), MNI (−8, 14, 46), *z*-score = 5.95, $P < 0.001$), bilaterally including parts of the gyrus rectus, anterior cingulate, medial superior frontal gyrus, and extending posteriorly to the supplementary motor area. The second significant area was located in the right hemisphere, partially covering the dorsolateral prefrontal cortex and extending to inferior frontal cortical regions and the precentral gyrus with a maximum in BA 44 (MNI (50, 8, 24), *z*-score = 4.7, $P < 0.0197$).

fMRI

Although the 1-back vs baseline contrast did not reveal any significant differences in activation, the 2-back vs baseline contrast revealed several areas of differential activation between the two groups. The patients showed significantly reduced activation compared with controls in two areas (Figure 1b, shown in blue). One of these areas comprised two distinct but clearly related clusters (cluster1: peak activation in BA 8, MNI (2, 26, 50), *z*-score = 4.35, $P < 1.19 \times 10^{-7}$; cluster2: peak activation in BA 6, MNI (−46, −2, 28), *z*-score = 4.12, $P < 0.00131$). These clusters included parts of the frontal operculum bilaterally, both the precentral gyri and the supplementary motor areas. They also reached some sections of the right dorsolateral prefrontal cortex and left basal ganglia. The other area was located in the cerebellum (peak activation in MNI coordinates (2, −56, −24), *z*-score = 5.96, $P < 1.91 \times 10^{-8}$).

In addition, the patients showed significant failure to deactivate in two clusters (Figure 1b, shown in orange). One of these extended over a large medial frontal area including, bilaterally, the gyrus rectus, anterior cingulate cortex, and parts of the superior medial frontal cortex and related frontomedial structures (peak activation in BA 11, MNI (−2, 38, −2), *z*-score = 4.91, $P < 1.78 \times 10^{-9}$). This cluster clearly overlapped with the region of volume reduction identified in the VBM analysis (Figure 1a). The other cluster where there was significant failure to deactivate was smaller, and contained parts of the hippocampal complex and neighbouring anterior temporal regions with a maximum activation in BA 48 (MNI (46, −8, −12), *z*-score = 4.04, $P < 0.000798$).

DTI

Owing to the excessive movement, only 25 patients and 28 controls could be included in this analysis. At $P = 0.01$ corrected, the major FA differences between the patients and controls were found in the corpus callosum (maximum in MNI space (22, 37, −1), $P < 0.00701$] (see Figure 2a). In particular, alterations were seen in the anterior portion of this structure, extending from below the genu to include the

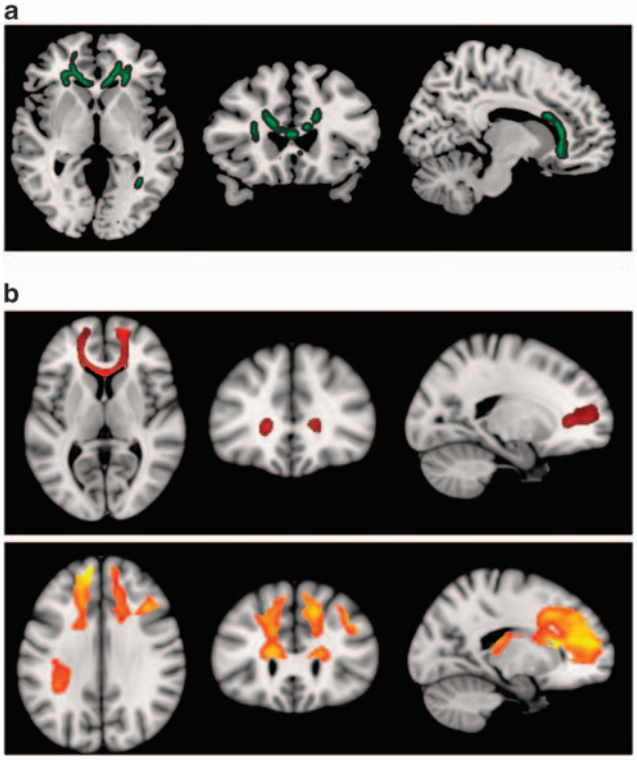

Figure 2 Diffusion tensor imaging (DTI) findings. Top panel (**a**) shows areas of significant fractional anisotropy (FA) reduction in the schizophrenic patients identified using TBSS thresholded at $P=0.01$. Bottom panels (**b**) show areas of structural connectivity that differed significantly between the schizophrenic patients and controls, on the basis of the seed placed in the genu of the corpus callosum (upper, shown in red), and the seeds placed in the body of the corpus callosum, right and left (lower, shown in orange). A threshold of $P=0.05$ corrected was used for this analysis. The right side of the images represents the left side of the brain.

rostral and anterior midbody. This area of significant difference also included the anterior corona radiata bilaterally (visible particularly in the left-hand figure).

A further anomalous region was located posteriorly in the splenium of the corpus callosum on the left, also involving the posterior thalamic radiation (including the optic radiation) and, to a lesser extent, the posterior corona radiata (maximum at MNI coordinates (−21, −83, 10), $P<0.007$).

To examine the relationship of the anterior callosal FA differences to the overlapping areas of structural and functional MRI abnormality in the medial prefrontal cortex, we performed a connectivity/tractography analysis (see Methods). For this, four ROIs were selected from an automatic parcellation of all areas with significant differences in FA at $P=0.01$. ROI#1 corresponded to the genu of the corpus callosum in the midline; ROI2# and ROI#3 were components of the left and right parts of the body of the corpus callosum anteriorly; ROI#4 was located within the left posterior thalamic radiation. In this analysis, we first applied a less conservative threshold of 0.05 rather than the 0.01 used in all other analyses: we expected higher levels of noise inherent to limitations in both the diffusion tensor model[38] and the tractography algorithm to reduce the statistical power of the connectivity analyses.

The three anteriorly placed seed regions (ROI#1, ROI#2 and ROI#3) showed significant connectivity differences between patients and controls, which affected principally a large expanse of the medial frontal cortex (see Figure 2b). It can be noted that there is a clear overlap between these results and areas showing failure to deactivate in fMRI and regions where there was volume reduction in VBM (Figures 1a and b). The seed placed in the left side of the body of the corpus callosum also showed differential connectivity with the left dorsolateral prefrontal cortex. The fourth seed, located posteriorly in the posterior thalamic radiation, did not result in any differential connectivity between the schizophrenic patients and the controls.

Repeating the analyses at a threshold of $P=0.01$ corrected had similar results, but the area of differential structural connectivity was less extensive. In particular, only the seed region ROI#3 in the right part of the body of the corpus callosum continued to show significant differences between patients and controls. These affected areas were very similar to those depicted in the lower panel of Figure 2b, but unilaterally on the right side of the brain.

Discussion

In this study, three different whole-brain voxel-based imaging techniques identified the medial prefrontal cortex as a prominent site of abnormality in schizophrenia. This region has not previously been a focus of interest in the disorder, although some post-mortem studies have noted microstructural abnormalities in the anterior cingulate cortex,[39] and it is an area where apparent hyperactivation,[12] and more recently failure of deactivation[14,15] has been found (see below). We also found evidence of convergent abnormality in the dorsolateral prefrontal cortex, which is an area of long-standing interest in schizophrenia. Here, however, the laterality was less consistent across techniques.

Our findings differ from two other studies that have applied whole-brain multimodal imaging to schizophrenia.[19,20] Calhoun *et al*.[19] examined 15 chronic schizophrenic patients and 15 controls using VBM and fMRI while performing an auditory oddball task. They used joint independent component analysis (jICA) of both modalities to determine areas of difference between the groups. Significant differences for VBM and fMRI were located in clearly different cortical regions, and there was no anatomical convergence. Lui *et al*.[20] carried out VBM on 68 patients with first-episode schizophrenia and 68 controls. Similar to our study, they found a cluster of grey

matter volume reduction in the anterior cingulate cortex (although on the right only), along with two other clusters in the right superior and right middle temporal gyri. However, when the authors used these three regions as seeds for a functional connectivity analysis using resting fMRI, no differences between the patients and the controls emerged.

Our findings are also different from those of other studies using single modalities of brain imaging. In particular, we found a considerably less extensive pattern of brain abnormality in the VBM and DTI analyses than in previous studies. On the one hand, this undoubtedly reflects our use of a conservative threshold of $P=0.01$ corrected. Thus, while two recent meta-analyses of VBM studies in schizophrenia[5,40] found, similar to this study, clusters of reduced volume in the medial prefrontal cortex and the dorsolateral prefrontal cortex, these were accompanied by other clusters, notably in the insula/inferior frontal cortex and medial temporal lobes. Some of these additional areas were also evident in our analysis using a threshold of $P=0.05$ (see Supplementary Material).

On the other hand, there are grounds for believing that VBM abnormality in schizophrenia may not be as widespread as originally thought. When the technique was originally introduced in 2000–2001,[41,42] it utilized a measure of grey matter concentration or density, the proportion of grey matter within a given voxel after spatial normalization of the images. Later, a modulated or 'optimized' method became available, which gives a more intuitive estimate of grey matter volume. Fornito *et al*.[40] meta-analysed studies using measures of grey matter concentration in schizophrenia and found clusters of significant reduction in the medial and lateral frontal cortex, temporal cortex and insula bilaterally. However, meta-analysis of studies using the volume measure resulted in a more restricted pattern of differences: changes in the temporal lobe and insula were no longer seen, and the largest areas of reduced volume were in the medial aspect of the left superior frontal gyrus plus the left orbitofrontal and fusiform regions.

DTI studies of schizophrenia have found evidence of abnormality in many different white matter areas, although these include the corpus callosum,[17] especially in recent studies.[21,43] Once again, however, there are grounds for believing that the true pattern may be more restrictive: Ellison-Wright and Bullmore[44] meta-analysed 15 studies which used a whole-brain voxel-based approach, and found that only two locations were consistently identified across studies. One of these was in the deep white matter of the left frontal lobe, close to the genu of the corpus callosum. The other area was in the left temporal lobe white matter. These areas are strikingly similar to those we found using a threshold of $P=0.01$ corrected.

The linchpin for the convergence of evidence in our study is the failure of deactivation in the medial frontal cortex, which was equally prominent at thresholds of $P=0.05$ or 0.01. One of the most important functional imaging findings to emerge in recent years has been that prefrontal cortex dysfunction in schizophrenia goes beyond any simple concept of hypofrontality, with a series of studies documenting areas of increased activation ('hyperfrontality') during performance of working memory tasks.[7–10] The leading interpretation of this finding has been that of cortical inefficiency: even when schizophrenic patients are able to perform a cognitive task normally, they have to 'work harder to keep up' with its demands, and this leads to a compensatory brain functional response characterized by greater and/or wider activation of the dorsolateral prefrontal cortex than in healthy subjects.[10,13] However, a meta-analysis of fMRI studies using the *n*-back task[12] casts doubts on this interpretation, as (a) hyperfrontality was found in the medial prefrontal cortex, not the dorsolateral and other lateral areas where hypofrontality was seen; and (b) this medial frontal area was not activated in the meta-analysis of either patients alone or controls alone. Subsequently, it has been argued that the hyperfrontality seen in the medial frontal cortex in schizophrenia actually represents a failure to deactivate[14] (because of 'reverse subtraction' from a high baseline, this can result in apparent hyperactivation, see Gusnard and Raichle[45]).

What is the function of this medial prefrontal area identified by multimodal imaging? As mentioned above, it includes, but is not limited to, the anterior cingulate cortex, an area which has been implicated in mood, attention, emotional regulation, error detection and decision making.[39,46] Perhaps more significantly, it corresponds closely to one of the two midline nodes of the default mode network, a system of brain regions that are active at rest but deactivate during performance of a wide range of attention demanding cognitive tasks.[16] The default mode network has been proposed to be involved in functions such as conceiving the perspectives of others, retrieving autobiographical memories and envisioning the future, processes that can be subsumed under a broad heading of mentation detached from the external world.[47] Going further, it has been argued that such functions underlie the experience and maintenance of one's sense of self.[48] A further possibility is that the default mode network underlies a state of 'watchfulness', a passive, low-level monitoring of the external environment for unexpected events in conditions when active attention is relaxed.[47] Any and all of these possibilities seem to have scope for explaining the symptoms of schizophrenia.

Conflict of interest

The authors declare no conflict of interest.

Acknowledgments

This work was supported by the Instituto de Salud Carlos III, Centro de Investigación en Red de Salud

Mental, CIBERSAM. Edith Pomarol-Clotet was supported by a Marie Curie European Reintegration Grant (MERG-CT-2004-511069). Raymond Salvador was supported by grants from the Instituto de Salud Carlos III (CP04/00322 and PI05/2693).

References

1 Van Horn JD, McManus IC. Ventricular enlargement in schizophrenia. A meta-analysis of studies of the ventricle:brain ratio (VBR). *Br J Psychiatry* 1992; **160**: 687–697.
2 Wright IC, Rabe-Hesketh S, Woodruff PW, David AS, Murray RM, Bullmore ET. Meta-analysis of regional brain volumes in schizophrenia. *Am J Psychiatry* 2000; **157**: 16–25.
3 McCarley RW, Wible CG, Frumin M, Hirayasu Y, Levitt JJ, Fischer IA *et al.* MRI anatomy of schizophrenia. *Biol Psychiatry* 1999; **45**: 1099–1119.
4 Honea R, Crow TJ, Passingham D, Mackay CE. Regional deficits in brain volume in schizophrenia: a meta-analysis of voxel-based morphometry studies. *Am J Psychiatry* 2005; **162**: 2233–2245.
5 Glahn DC, Laird AR, Ellison-Wright I, Thelen SM, Robinson JL, Lancaster JL *et al.* Meta-analysis of gray matter anomalies in schizophrenia: application of anatomic likelihood estimation and network analysis. *Biol Psychiatry* 2008; **64**: 774–781.
6 Hill K, Mann L, Laws KR, Stephenson CM, Nimmo-Smith I, McKenna PJ. Hypofrontality in schizophrenia: a meta-analysis of functional imaging studies. *Acta Psychiatr Scand* 2004; **110**: 243–256.
7 Manoach DS, Press DZ, Thangaraj V, Searl MM, Goff DC, Halpern E *et al.* Schizophrenic subjects activate dorsolateral prefrontal cortex during a working memory task, as measured by fMRI. *Biol Psychiatry* 1999; **45**: 1128–1137.
8 Callicott JH, Bertolino A, Mattay VS, Langheim FJ, Duyn J, Coppola R *et al.* Physiological dysfunction of the dorsolateral prefrontal cortex in schizophrenia revisited. *Cereb Cortex* 2000; **10**: 1078–1092.
9 Tan HY, Sust S, Buckholtz JW, Mattay VS, Meyer-Lindenberg A, Egan MF *et al.* Dysfunctional prefrontal regional specialization and compensation in schizophrenia. *Am J Psychiatry* 2006; **163**: 1969–1977.
10 Callicott JH, Mattay VS, Verchinski BA, Marenco S, Egan MF, Weinberger DR. Complexity of prefrontal cortical dysfunction in schizophrenia: more than up or down. *Am J Psychiatry* 2003; **160**: 2209–2215.
11 Manoach DS. Prefrontal cortex dysfunction during working memory performance in schizophrenia: reconciling discrepant findings. *Schizophr Res* 2003; **60**: 285–298.
12 Glahn DC, Ragland JD, Abramoff A, Barrett J, Laird AR, Bearden CE *et al.* Beyond hypofrontality: a quantitative meta-analysis of functional neuroimaging studies of working memory in schizophrenia. *Hum Brain Mapp* 2005; **25**: 60–69.
13 Tan HY, Callicott JH, Weinberger DR. Dysfunctional and compensatory prefrontal cortical systems, genes and the pathogenesis of schizophrenia. *Cereb Cortex* 2007; **17**(Suppl 1): i171–i181.
14 Pomarol-Clotet E, Salvador R, Sarro S, Gomar J, Vila F, Martinez A *et al.* Failure to deactivate in the prefrontal cortex in schizophrenia: dysfunction of the default mode network? *Psychol Med* 2008; **38**: 1185–1193.
15 Whitfield-Gabrieli S, Thermenos HW, Milanovic S, Tsuang MT, Faraone SV, McCarley RW *et al.* Hyperactivity and hyperconnectivity of the default network in schizophrenia and in first-degree relatives of persons with schizophrenia. *Proc Natl Acad Sci USA* 2009; **106**: 1279–1284.
16 Raichle ME, MacLeod AM, Snyder AZ, Powers WJ, Gusnard DA, Shulman GL. A default mode of brain function. *Proc Natl Acad Sci USA* 2001; **98**: 676–682.
17 Kubicki M, McCarley R, Westin CF, Park HJ, Maier S, Kikinis R, *et al.* A review of diffusion tensor imaging studies in schizophrenia. *J Psychiatr Res* 2007; **41**: 15–30.
18 Lim KO. Connections in schizophrenia. *Am J Psychiatry* 2007; **164**: 995–998.
19 Calhoun VD, Adali T, Giuliani NR, Pekar JJ, Kiehl KA, Pearlson GD. Method for multimodal analysis of independent source differences in schizophrenia: combining gray matter structural and auditory oddball functional data. *Hum Brain Mapp* 2006; **27**: 47–62.
20 Lui S, Deng W, Huang X, Jiang L, Ma X, Chen H *et al.* Association of cerebral deficits with clinical symptoms in antipsychotic-naive first-episode schizophrenia: an optimized voxel-based morphometry and resting state functional connectivity study. *Am J Psychiatry* 2009; **166**: 196–205.
21 Miyata J, Hirao K, Namiki C, Fujiwara H, Shimizu M, Fukuyama H *et al.* Reduced white matter integrity correlated with cortico-subcortical gray matter deficits in schizophrenia. *Schizophr Res* 2009; **111**: 78–85.
22 Kalus P, Buri C, Slotboom J, Gralla J, Remonda L, Dierks T *et al.* Volumetry and diffusion tensor imaging of hippocampal subregions in schizophrenia. *Neuroreport* 2004; **15**: 867–871.
23 Kalus P, Slotboom J, Gallinat J, Federspiel A, Gralla J, Remonda L *et al.* New evidence for involvement of the entorhinal region in schizophrenia: a combined MRI volumetric and DTI study. *Neuroimage* 2005; **24**: 1122–1129.
24 Kalus P, Slotboom J, Gallinat J, Wiest R, Ozdoba C, Federspiel A *et al.* The amygdala in schizophrenia: a trimodal magnetic resonance imaging study. *Neurosci Lett* 2005; **375**: 151–156.
25 Mechelli A, Price CJ, Friston KJ, Ashburner J. Voxel-based morphometry of the human brain: methods and applications. *Curr Med Imaging Rev* 2005; **1**: 1–25.
26 Smith SM, Jenkinson M, Johansen-Berg H, Rueckert D, Nichols TE, Mackay CE *et al.* Tract-based spatial statistics: voxelwise analysis of multi-subject diffusion data. *Neuroimage* 2006; **31**: 1487–1505.
27 Smith SM, Jenkinson M, Woolrich MW, Beckmann CF, Behrens TE, Johansen-Berg H *et al.* Advances in functional and structural MR image analysis and implementation as FSL. *Neuroimage* 2004; **23**(Suppl 1): S208–S219.
28 Smith SM. Fast robust automated brain extraction. *Hum Brain Mapp* 2002; **17**: 143–155.
29 Smith SM, Nichols TE. Threshold-free cluster enhancement: addressing problems of smoothing, threshold dependence and localisation in cluster inference. *Neuroimage* 2009; **44**: 83–98.
30 Gevins A, Cutillo B. Spatiotemporal dynamics of component processes in human working memory. *Electroencephalogr Clin Neurophysiol* 1993; **87**: 128–143.
31 Andersson JLR, Jenkinson M, Smith S. Non-linear optimisation. *FMRIB Technical Report TR07JA1* 2007; http://www.fmrib.ox.ac.uk/analysis/techrep.
32 Andersson JLR, Jenkinson M, Smith S. Non-linear optimisation, aka Spatial nornalisation. *FMRIB Technical Report TR07JA2* 2007; http://www.fmrib.ox.ac.uk/analysis/techrep.
33 Rueckert D, Sonoda L, Hayes C, Hill D, Leach M, Hawkes D. Non-rigid registration using free-form deformations: application to breast MR images. *IEEE Transactions on Medical Imaging* 1999; **18**: 712–721.
34 Iturria-Medina Y, Canales-Rodriguez EJ, Melie-Garcia L, Valdes-Hernandez PA, Martinez-Montes E, Aleman-Gomez Y *et al.* Characterizing brain anatomical connections using diffusion weighted MRI and graph theory. *Neuroimage* 2007; **36**: 645–660.
35 Iturria-Medina Y, Sotero RC, Canales-Rodriguez EJ, Aleman-Gomez Y, Melie-Garcia L. Studying the human brain anatomical network via diffusion-weighted MRI and Graph Theory. *Neuroimage* 2008; **40**: 1064–1076.
36 Nelson HE, Willison JR. *The Revised National Adult Reading Test*. NFER-Nelson: Windsor, Berkshire, 1991.
37 Del Ser T, Gonzalez-Montalvo JI, Martinez-Espinosa S, Delgado-Villapalos C, Bermejo F. Estimation of premorbid intelligence in Spanish people with the Word Accentuation Test and its application to the diagnosis of dementia. *Brain Cogn* 1997; **33**: 343–356.
38 Frank LR. Characterization of anisotropy in high angular resolution diffusion-weighted MRI. *Magn Reson Med* 2002; **47**: 1083–1099.
39 Fornito A, Yucel M, Dean B, Wood SJ, Pantelis C. Anatomical abnormalities of the anterior cingulate cortex in schizophrenia: bridging the gap between neuroimaging and neuropathology. *Schizophr Bull* 2009; **35**: 973–993.
40 Fornito A, Yucel M, Patti J, Wood SJ, Pantelis C. Mapping grey matter reductions in schizophrenia: an anatomical likelihood

estimation analysis of voxel-based morphometry studies. *Schizophr Res* 2009; **108**: 104–113.
41 Ashburner J, Friston KJ. Voxel-based morphometry—the methods. *Neuroimage* 2000; **11**: 805–821.
42 Good CD, Johnsrude IS, Ashburner J, Henson RN, Friston KJ, Frackowiak RS. A voxel-based morphometric study of ageing in 465 normal adult human brains. *Neuroimage* 2001; **14**: 21–36.
43 Rotarska-Jagiela A, Schonmeyer R, Oertel V, Haenschel C, Vogeley K, Linden DE. The corpus callosum in schizophrenia-volume and connectivity changes affect specific regions. *Neuroimage* 2008; **39**: 1522–1532.
44 Ellison-Wright I, Bullmore E. Meta-analysis of diffusion tensor imaging studies in schizophrenia. *Schizophr Res* 2009; **108**: 3–10.
45 Gusnard DA, Raichle ME. Searching for a baseline: functional imaging and the resting human brain. *Nat Rev Neurosci* 2001; **2**: 685–694.
46 Devinsky O, Morrell MJ, Vogt BA. Contributions of anterior cingulate cortex to behaviour. *Brain* 1995; **118**: 279–306.
47 Buckner RL, Andrews-Hanna JR, Schacter DL. The brain's default network: anatomy, function, and relevance to disease. *Ann N Y Acad Sci* 2008; **1124**: 1–38.
48 Gusnard DA. Being a self: considerations from functional imaging. *Conscious Cogn* 2005; **14**: 679–697.

Supplementary Information accompanies the paper on the Molecular Psychiatry website (http://www.nature.com/mp)